Molecular Therapy
Nucleic Acids
Original Article

Trans-acting aptazyme for conditional gene knockdown in eukaryotic cells

Shan Zhou,[1,2] Meiyi Chen,[1] Yi Yuan,[1] Yan Xu,[1] Qinlin Pu,[1] Xilei Ai,[1] Shuai Liu,[1] Feng Du,[1] Xin Huang,[1] Juan Dong,[1] Xin Cui,[1] and Zhuo Tang[1]

[1]Natural Products Research Center, Chengdu Institution of Biology, Chinese Academy of Sciences, Chengdu 610041, P.R. China; [2]University of Chinese Academy of Sciences, Beijing 100049, P.R. China

***Trans*-acting hammerhead ribozyme inherits the advantages of being the smallest and best-characterized RNA-cleaving ribozyme, offering high modularity and the ability to cleave any desired sequence without the aid of any protein, as long as the target sequence contains a cleavage site. However, achieving precise control over the *trans*-acting hammerhead ribozyme would enable safer and more accurate regulation of gene expression. Herein, we described an intracellular selection of hammerhead aptazyme that contains a theophylline aptamer on stem II based on toxin protein IbsC. Based on the intracellular selection, we obtained three new *cis*-acting hammerhead aptazymes. Moreover, the corresponding *trans*-acting aptazymes could be efficiently induced by theophylline to knock down different targeted genes in eukaryotic cells. Notably, the best one, T195, exhibited a ligand-dependent and dose-dependent response to theophylline, and the cleavage efficiency could be enhanced by incorporating multiplex aptazymes.**

INTRODUCTION

Ribozymes are catalytic RNA molecules that can catalyze a chemical reaction. The hammerhead ribozyme (HHRz) is the smallest and best-characterized self-cleaving ribozyme, which catalyzes the hydrolysis of phosphodiester linkage through nucleophilic attack by the 2′-hydroxyl of cleavage site.[1,2] The name "hammerhead" derives from its two-dimensional structure, featuring three base-paired stems (designated as I–III) and a conserved core region responsible for cleavage (refer to Figure 1A).[2] As a critical member of self-cleaving ribozymes, the hammerhead ribozyme was first discovered in viroids, and it could be the most widespread ribozyme family as it has been found across all domains of life.[3] Based on the unique secondary structure, hammerhead ribozymes have been engineered to catalyze the intermolecular RNA cleavage via splitting loop III (Figure 1B).[1] The *trans*-acting hammerhead ribozyme recognizes RNA substrate through two binding arms and cleaves it after triplet NUH↓ (N is any base, and H is A, C, or U, Figure 1B). By altering the binding sequence according to the targeted mRNA, hammerhead ribozyme can selectively cleave virtually any mRNA target. However, small interfering RNA (siRNA) and antisense oligonucleotides achieve more efficient gene knockdown through the assistance of the RISC complex and RNase H, respectively. Though the efficiencies of *trans*-acting ribozymes are not efficient as siRNA, ribozymes remain attractive therapeutic agents due to their specificity of target recognition and precise cleavage, without any reported "off-target" effects.[4] As the first gene therapy agent to reach clinical trials, hammerhead ribozyme remains the only reported agent tested in a randomized, double-blind, cell-delivered clinical phase II trial for HIV-1 infection.[5] Though two phase II trials based on hammerhead ribozyme have failed so far due to the inefficient *trans*-cleavage activity *in vivo*, the research results show that the hammerhead ribozyme is safe and biologically active in individuals with HIV-1 infection.[6] To improve the intracellular activity of the hammerhead ribozyme, a direct intracellular selection method has been developed by our group to evolve hammerhead variants based on *trans*-cleavage mode via using a toxin gene as the reporter.[7] The selected variants showed an enhanced ability for intracellular gene silencing toward various RNA targets in cell and zebrafish embryos. However, the precise control of gene knockdown induced by *trans*-acting hammerhead ribozyme has not been realized.

In contrast, the *cis*-acting hammerhead ribozyme has been utilized to construct artificial riboswitches, also termed as aptazymes, exhibiting the huge potential to be a transgene expression regulator.[8–16] As shown in Figure 1C, the hammerhead aptazyme is chimeric RNA that consists an aptamer domain, a ribozyme domain, and a linker module, which can modulate its self-cleavage by a specific ligand. The binding of ligand with aptamer domain can stabilize the catalytic core of ribozyme via the linker module and promote the RNA self-cleavage, thus downregulating gene expression (Figure 1C). Unfortunately, we cannot directly transform the *cis*-acting aptazymes into *trans*-acting gene silencing tools. Since the interaction between loop I and loop II in hammerhead pseudoknot tertiary structure has been proved to be very important for the *cis*-cleavage in the cell (Figure 1A), most reported aptazymes that can work in prokaryotic cells or in eukaryotic cells were constructed by appending different aptamers to stem III of hammerhead ribozyme (Figure 1C). Therefore, to get the *trans*-acting hammerhead aptazyme, we need to move the

Received 13 April 2023; accepted 11 July 2023;
https://doi.org/10.1016/j.omtn.2023.07.014.

Correspondence: Zhuo Tang, Natural Products Research Center, Chengdu Institution of Biology, Chinese Academy of Sciences, Chengdu 610041, P.R. China.
E-mail: tangzhuo@cib.ac.cn

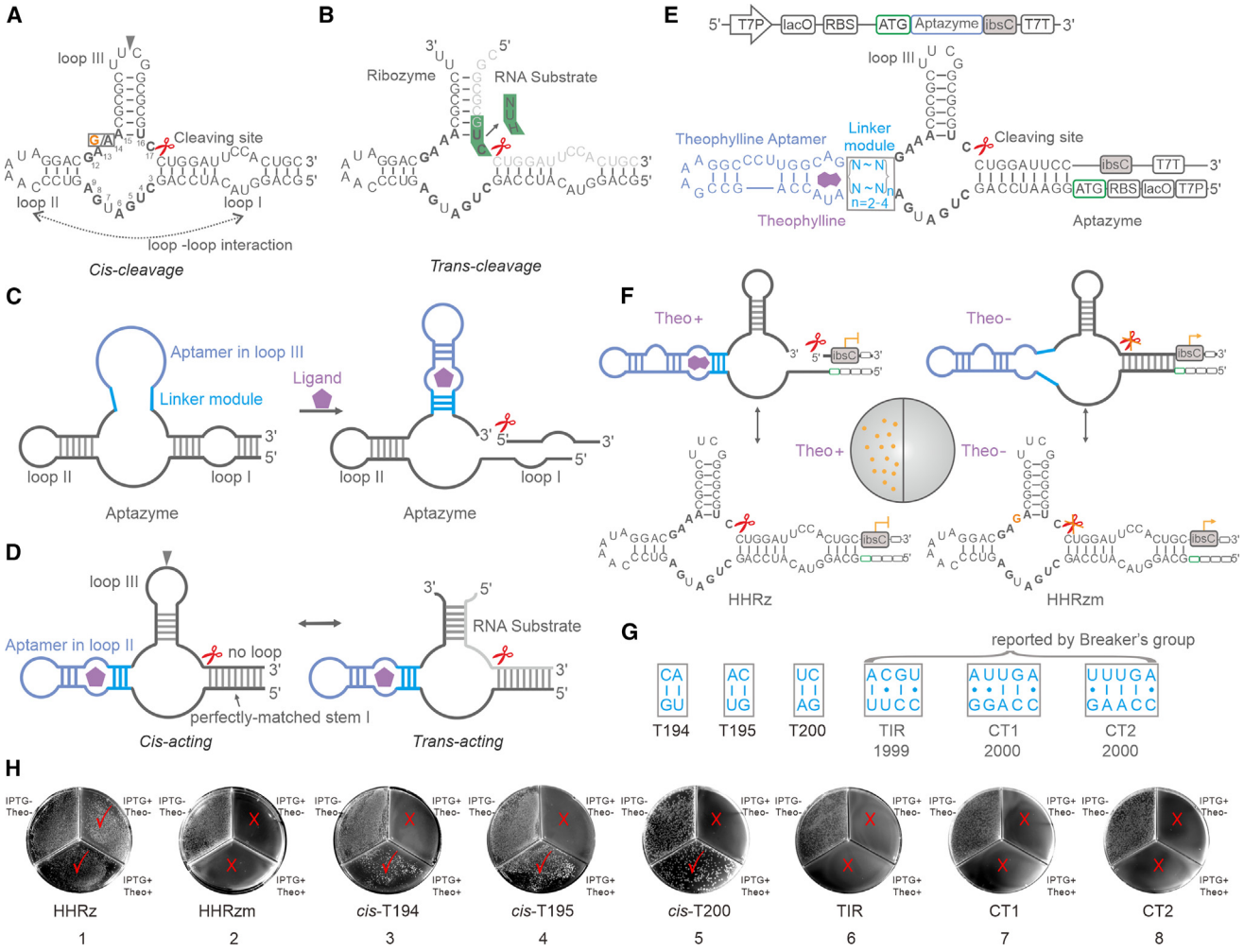

Figure 1. Intracellular selection of hammerhead aptazyme that contains an aptamer on stem II

(A) *Cis*-cleavage of hammerhead ribozyme; bold letters indicate the catalytic core, A14 mutated G14 indicates the inactivated hammerhead ribozyme, red scissor indicates the self-cleavage site, gray arrow indicates the bisection of the hammerhead ribozyme, and gray two-directional arrow indicates the interaction between loop I and loop II. (B) *Trans*-cleavage of hammerhead ribozyme, where green indicates the cleavage triplet NUH↓. (C) The general structure of the hammerhead aptazyme; indigo represents the aptamer domain, blue represents the linker module, and the ligand binds to the aptamer to help maintain the active conformation to promote self-cleavage. (D) Hammerhead aptazyme that contains an aptamer on stem II, which can be converted into *trans*-cleaving hammerhead aptazyme. (E) Construction of selection vector based on toxin protein lbsC. (F) Self-cleavage activity of aptazyme with and without theophylline is similar to that of HHRz and HHRzm, respectively. (G) Linker module of different hammerhead aptazymes. (H) Results of different viability for *E. coli* transferred with different aptazymes on the solid medium added with and without theophylline. The concentration of ampicillin is 100 μg/mL, IPTG is 1 mM, and theophylline is 1 mM.

aptamer sequence from stem III to stem II without affecting the intracellular cleaving ability of ribozyme (Figure 1D). A few aptazymes that can work in yeast were constructed by appending aptamers to stem II, and their cleavage activity was dependent on the interaction between loop I and loop II, and thus, they cannot be converted into *trans*-acting aptazymes directly.[9,13] Herein, we described an intracellular selection of hammerhead aptazyme that contains an aptamer on stem II, through which new *cis*-acting hammerhead aptazymes were obtained. And, the corresponding *trans*-acting aptazymes could be efficiently induced by theophylline to knock down different targeted genes in eukaryotic cells.

RESULTS

Intracellular selection of hammerhead aptazyme that contains an aptamer on stem II

We chose theophylline as the exogenous ligand of hammerhead aptazyme because it is a commonly used medicine for the treatment of chronic asthma with a good safety profile.[17] As shown in Figure 1E, the theophylline aptamer was designed to replace loop II and connected to the catalytic core of ribozyme through a linker module. Meanwhile, the loop I was removed by us, leaving a neat stem I, since the *trans*-acting ribozyme recognizes the targeted RNA sequence by forming perfectly matched duplexes (Figure 1D). To achieve

intracellular selection, our newly constructed hammerhead aptazyme was inserted to the 5′ end of a toxin gene *ibsC* that would be expressed in the *E. coli* by recombinant plasmids. IbsC is a 19-amino-acid toxin protein originated from *E. coli*, and its overexpression would compromise the integrity of bacterial membrane and result in bacteria cell death.[18–20] Therefore, if the intracellular hammerhead aptazymes work in the presence of theophylline, the RNA self-cleavage would prevent the expression of *ibsC*, thus allowing bacteria to survive (Figures 1E and S1). To test the feasibility of this strategy, a wild-type hammerhead ribozyme was inserted between ribosomal binding site and open reading frame of *ibsC* to imitate the active aptazyme with theophylline, while the inactive hammerhead ribozyme (HHRzm with an A to G mutation at position 14 in the catalytic core) was inserted at the same position to imitate active aptazyme without theophylline (Figure 1F). As shown in the culture plates of Figure 1H, host cells survived on agar plate 1 instead of plate 2 when the transcription of *ibsC* was induced by isopropyl β-D-thiogalactoside (IPTG), revealing that the self-cleavage of active HHRz in mRNA sequences suppressed the expression of the downstream toxin gene.[7,16] Therefore, a hammerhead aptazymes pool containing 2–4 base pairs of random linker modules (Figure 1E) was synthesized and constructed into the recombinant plasmids and transferred into *E. coli*. We collected colonies that survived on the resistant culture plate with 100 μg/mL ampicillin, 1 mM IPTG, and 1 mM theophylline. Then we compared the growth performance of these candidates on agar plates with or without theophylline (Figure S2). Finally, three stem II-based aptazymes (T194, T195, and T200 in Figure 1G) were confirmed to help host cells survive in the presence of theophylline (plates 3, 4, and 5 in Figure 1H). Next, we introduced the A to G mutation at position 14 in the catalytic cores of T194, T195, and T200 respectively to inactivate the function of aptazymes. Under IPTG induction, these mutant aptazymes (T194m, T195m, and T200m) failed to help host cells survive in the presence of theophylline (Figure S3), confirming that the three aptazymes obtained through intracellular selection can help the host cell survive through self-cleavage in the presence of theophylline. Furthermore, hosts containing hammerhead aptazymes (T194, T195, and T200) grew better at higher concentrations of theophylline (Figure S4), suggesting these stem II-based aptazymes are regulated by theophylline in a dose-dependent manner. Breaker's group has reported several stem II-based aptazymes (TIR, CT1, and CT2, shown in Figure 1G) obtained through *in vitro* selection,[21,22] and we inserted them into our recombinant plasmids to evaluate their performance in prokaryotic cells. Unfortunately, bacteria expressing those *in vitro*-selected aptazymes failed to survive in the presence of theophylline (plates 6, 7, and 8 in Figure 1H), indicating that the activities of aptazymes *in vitro* are not necessarily correlated with their performance in the cellular environment.

As the linker module of all selected aptazymes was composed of two matched base pairs (T194, T195, and T200, as shown in Figure 1G), we wondered whether any two base-pair duplexes can be successfully applied as a linker to construct the theophylline aptazymes. Therefore, we constructed several aptazymes containing arbitrary two base-pair linkers, none of which were able to support bacterial survival in the same manner as the selected aptazymes (Figure S5).

Intracellular verification of *cis*-cleaving ability of hammerhead aptazymes by mCherry fluorescent protein

Though we successfully obtained three stem II-based hammerhead aptazymes through intracellular selection, using the IbsC-based cell survival assay, it is hard to quantify their intracellular regulating ability. Therefore, to get the accurate switching ability of the obtained aptazymes with and without theophylline, the reporting protein IbsC was replaced with a low-background red fluorescent protein mCherry (Figures 2A and S6). The fluorescent signals of *E. coli* cells expressing aptazymes (T200, T194, and T195) reduced significantly in the presence theophylline (1.25 mM), providing 1.81-, 2.22-, and 2.84-fold repression of mCherry expression, respectively (Figures 2B and 2C). And the response of T195 and mutant ribozyme HHRzm to different concentrations of theophylline was studied by flow cytometry, respectively. The results showed that T195 was highly sensitive to the exogenous regulator from 10 μM to 5 mM, while HHRzm had a slight reaction to theophylline, which may be due to theophylline toxicity (Figures 2D and S7).

Verification of *trans*-cleaving ability of hammerhead aptazymes *in vitro*

Since we have obtained the *cis*-acting hammerhead aptazymes through intracellular selection, their *trans*-acting capability was investigated subsequently. We conducted *in vitro* cleaving assays to evaluate cleavage ability of aptazymes in the presence and absence of theophylline (Figure 2E). The synthesized 3′FAM-modified RNA substrate were cleaved by *trans*-acting ribozyme and aptazymes respectively, and the *in vitro* cleavage reactions proceeded under simulated physiological condition.[23] Excitingly, as shown in Figure 2F, the presence of theophylline increased the *trans*-cleavage efficiency of T194 and T195 by 1.13 times (lanes 3 and 4) and 6.22 times (lanes 5 and 6), respectively. In contrast, the *trans*-cleavage efficiency of wild-type HHR decreased slightly (lanes 1 and 2). Furthermore, the cleavage capacity of *trans*-acting aptazyme T195 increased in a dose-dependent manner with increasing theophylline concentrations (Figure 2G), indicating that T195 can effectively respond to theophylline. The cleavage kinetics data in Figures 2H and S8 also revealed that the observed rate constant (k_{obs}) of T195 in the presence of theophylline was 6.1 times higher than that in the absence of theophylline (0.061 min^{-1} versus 0.010 min^{-1}). Taken together, the data demonstrate that stem II-based *cis*-acting hammerhead aptazymes obtained through intracellular selection can be converted into *trans*-acting aptazymes, and their *trans*-cleavage activity can be regulated by theophylline, just like their *cis*-cleavage activity. These results verify the feasibility of our strategy for selecting new *trans*-cleavage hammerhead aptazymes.

Intracellular verification of *trans*-cleaving ability of hammerhead aptazymes by endogenous proteins

After confirming the *trans*-cleaving ability of aptazymes *in vitro*, we proceeded to assess their performances in eukaryotic cells. To achieve

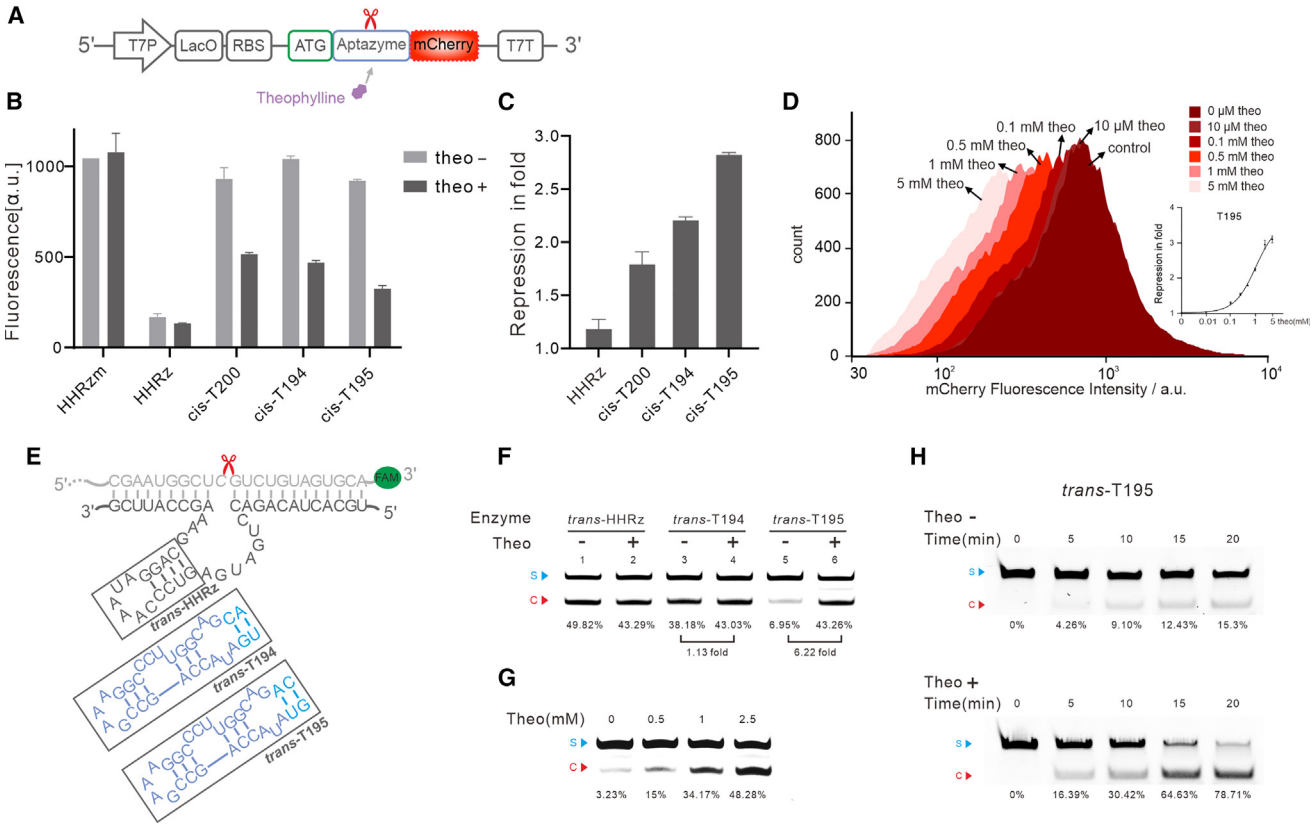

Figure 2. Verification of *cis*-cleaving ability of hammerhead aptazymes by mCherry fluorescent protein in prokaryotic cells and verification of *trans*-cleaving ability of hammerhead aptazymes *in vitro*

(A) Construction of *cis*-cleaving ability verification vector based on fluorescence protein mCherry. (B) mCherry fluorescence of the *E. coli* transferred with ribozymes or aptazymes in the liquid LB medium in the presence and absence of 1.25 mM theophylline. *E. coli* containing ribozyme or aptazymes was cultivated to OD600 0.3 and induced by 1 mM IPTG for 18 h and then analyzed by FCM. Results were expressed as mean ± SD. (C) Repression in fold of (B). (D) FCM histograms of the *E. coli* transferred with aptazyme T195 in the liquid LB medium added with different concentrations of theophylline. Theophylline concentrations were 0, 0.01, 0.1, 0.25, 0.5, 1, 2.5, and 5 mM. (E) The cleavage model of *trans*-acting ribozyme and *trans*-acting aptazymes. (F) PAGE analysis of 3′FAM-labeled *trans*-cleaving result of HHRz, T194, and T195. HHRz was set as the positive control. The reaction is performed in 50 mM Tris-HCl (pH 7.5) buffer containing 1 mM $MgCl_2$, 150 mM KCl, and 1 mg/ml BSA at 37°C for 10 min with or without 2.5 mM theophylline. "S" stands for "substrate," and "C" stands for "cleavage product." (G) PAGE analysis of FAM-labeled *trans*-cleaving result of T195 at different theophylline concentrations. The reaction buffer was the same as in (F). The reaction time was 10 min. Theophylline concentrations were 0, 0.5, 1, and 2.5 mM. (H) Cleavage efficiency of *trans*-acting T195 in the presence and absence of theophylline under different times. The reaction buffer was the same as in (F). The theophylline concentration was 1 mM.

this, we directly applied T194 and T195 to eukaryotic cells to knock down endogenous genes. In mammalian cells, the NF-κB family of transcription factors are composed of five distinct subunits, RelA (p65), c-Rel, RelB, p50 (NF-κB1), and p52 (NF-κB2).[24] The activation of NF-κB is often encountered in tumor cells and contributes to aggressive tumor growth and resistance to chemotherapy during cancer treatment.[25] Therefore, p65 was selected as the first endogenous target of our stem II-based hammerhead aptazymes. The corresponding T194 and T195 were designed to cleave the *RELA* (name of the gene corresponding to p65 protein) mRNA, and we use the U6-tRNA processing system, which is a highly efficient promoter capable of accurately and cleanly expressing RNA to enhance the expression of *trans*-ribozyme in eukaryotic cells (Figures 3A, S9, and S10).[26] We constructed plasmid vectors and transfected them into MCF-7 cells respectively. 24 h after transfection, MCF-7 cells were harvested and analyzed by western blot (WB). As shown in Figures 3B and S11, we found that both T194 and T195 can downregulate the expression of *RELA* in the presence of 1 mM theophylline, while no decrease of p65 proteins was observed with or without theophylline in the cell expressing inactive hammerhead ribozymes (negative control). Meanwhile, we investigated the knockdown ability of *trans*-acting aptazymes on *RELA* mRNA level by RT-qRCR. As shown in Figures 3B and 3C, the RT-qRCR results were consistent with results at the translational level, revealing that T195 provided a better knockdown effect induced by theophylline. After transfection, T195 effectively downregulated p65 proteins within 12 h and reached the highest level at 24 h, and then the knockdown efficiency decreased over time (Figure S12). Meanwhile, we introduced the A to G mutation at position 14 in the

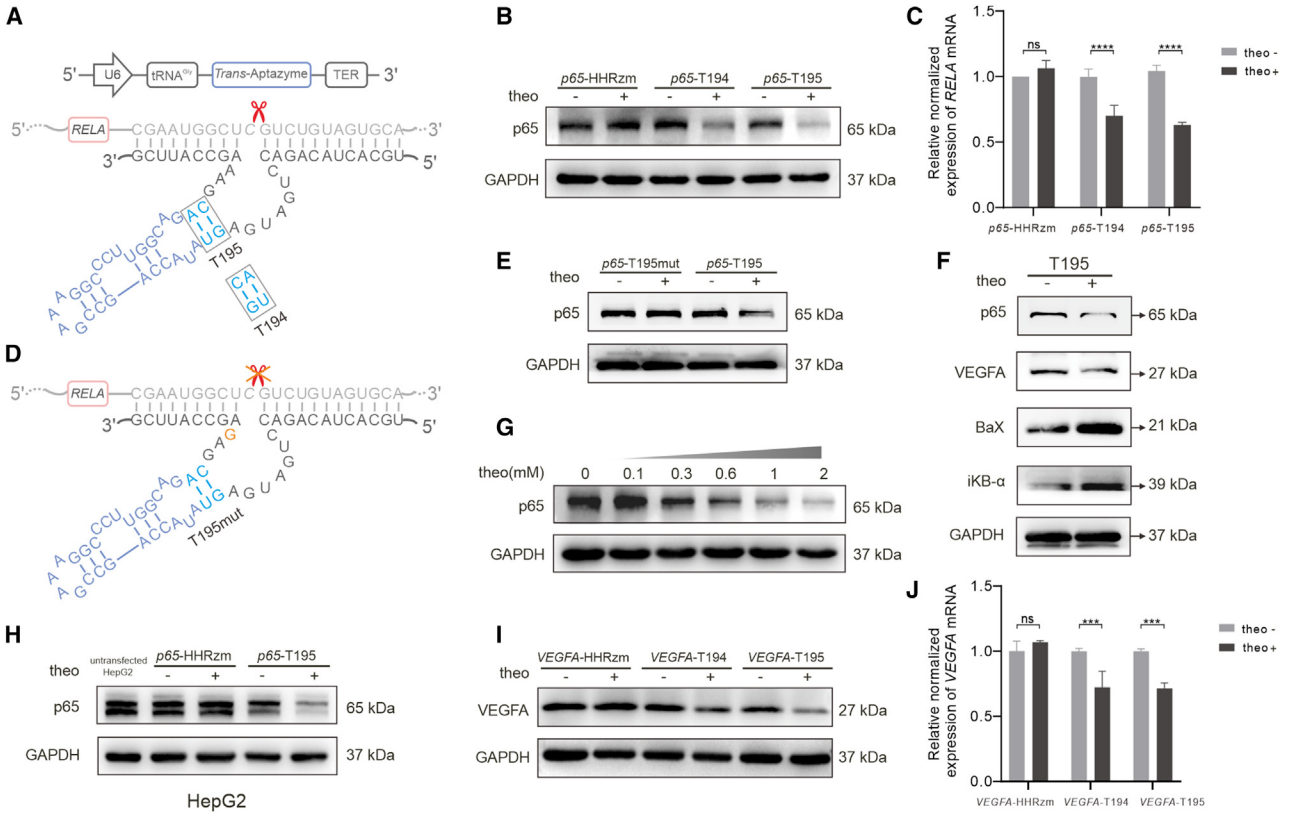

Figure 3. Intracellular verification of *trans*-cleaving ability of hammerhead aptazymes by endogenous proteins

(A) Construction of *trans*-cleaving ability verification vector. The secondary structure of different *trans*-aptazymes targeting *RELA*. (B) p65 protein decrease of cells transfected into with *trans*-aptazymes under 1 mM theophylline by WB. (C) p65 protein decrease of cells transfected into with *trans*-aptazymes under 1 mM theophylline by qRT-PCR. Compared with the corresponding aptazymes transfected into cells in the absence of theophylline, ****$p < 0.0001$. (D) The secondary structure of mutated *trans*-aptazyme T195m targeting *RELA*. (E) p65 protein decrease of cells transfected into with *trans*-aptazyme T195 and its mutated T195m by WB. (F) Phenotype study of the p65 knocked down cells. Western blot analysis was performed to determine the levels of NF-kB inhibitor alpha (IkB-a), apoptosis-related proteins (Bax), and angiogenesis-related proteins (VEGF) in the MCF-7 cells expressing *trans*-T195 after 24 h in the presence of theophylline. (G) p65 protein decrease of cells transfected with *trans*-T195 under different concentrations of theophylline by WB. Theophylline concentrations are 0, 0.1, 0.3, 0.6, 1, and 2 mM. (H) p65 protein decrease of HepG2 cells transfected with *trans*-T195 under 1 mM theophylline by WB. (I) VEGFA protein decrease of cells transfected with *trans*-aptazymes under 1 mM theophylline by WB. (J) VEGFA protein decrease of cells transfected with *trans*-aptazymes under 1 mM theophylline by qRT-PCR. Compared with the corresponding aptazymes transfected into cells in the absence of theophylline, ***$p < 0.001$.

catalytic core of T195 to inactivate the function of aptazyme, named T195mut (Figure 3D). We used T195 as positive control and its mutated T195m as negative control to investigate whether T195 could downregulate the expression of *RELA* under theophylline regulation. As shown in Figures 3E and S13, T195 could obviously knock down p65 in the presence theophylline, while T195mut could not knock down p65 in the presence or absence of theophylline. Furthermore, to investigate the influence of p65 knockdown on cells, we performed NF-kB signal-related protein analysis. As shown in Figures 3F and S14, cytoplasmic NF-kB inhibitor IkB[27] and proapoptotic protein Bax were upregulated, and VEGF[28] was downregulated, further confirming the downregulation of NF-kB caused by *trans*-aptazyme T195 of p65 in MCF-7 cells. As expected, the knockdown ability of *trans*-acting T195 was regulated by theophylline in a dose-dependent manner (Figures 3G and S15). Furthermore, the theophylline-triggered downregulation of p65 proteins by genetically encoded T195 was also verified in HepG2 cells (Figures 3H and S16). Breaker's group has reported two stem-II-based hammerhead aptazymes (H8 and H14) obtained through rational design (Figure S17), which revealed *trans*-cleaving activity upon theophylline *in vitro*.[29,30] Thus, their knockdown ability on the same targeted sequence in eukaryotic cells was evaluated by expressing them in MCF-7 cells too. As shown in Figure S17, there were no significant p65 knockdowns observed in cells expressing H8 and H14, indicating that the *trans*-acting aptazymes obtained *in vitro* cannot function properly in cancer cells.

To further investigate the generalizability of stem II-based hammerheads aptazymes to different targets, we applied our *trans*-acting aptazymes to regulate the expression of vascular endothelial growth factor-A (VEGFA), which participates in many signal pathways and

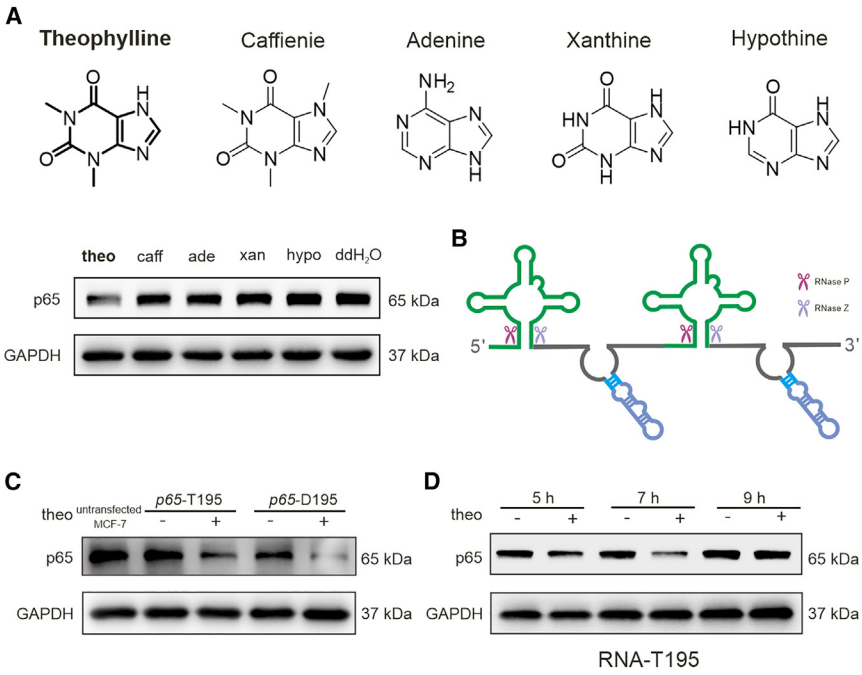

Figure 4. Further optimization of the *trans*-cleaving ability of hammerhead aptazyme

(A) p65 protein decrease of cells transfected with *trans*-T195 under different small molecules by WB. "theo" indicates theophylline, "caff" indicates caffeine, "ade" indicates adenine, "xan" indicates xanthine, and "hypo" indicates hypoxanthine. (B) The secondary structure of two $tRNA^{Gly}$-*trans*-cleaving hammerhead aptazyme elements. The tRNA precursors (pre-tRNAs) are cleaved at specific sites in eukaryotes by RNase P and RNase Z[26]. (C) p65 protein decrease of cells transfected with T195 and D195 under 1 mM theophylline by WB. (D) p65 protein decrease of cells transfected with *trans*-T195 RNA under 1 mM theophylline. 5, 7, and 9 h post transfection, cells were analyzed by WB.

plays a key role in tumor angiogenesis. In addition, *VEGFA* is highly expressed in a variety of tumor tissues and cells as a cancer-promoting gene, which is closely related to the occurrence, development, metastasis, and prognosis of tumors.[31] Therefore, the corresponding T194 and T195 were designed and constructed to cleave the *VEGFA* mRNA (Figure S18), and we found that T195 once again showed a better ability to knock down *VEGFA* with 1 mM theophylline in MCF-7 cells, while no decrease of VEGFA proteins was observed with or without theophylline in the cell expressing inactive hammerhead ribozymes (Figures 3I and S19). The knockdown ability of *trans*-acting aptazymes on *VEGFA* mRNA level by RT-qRCR was consistent with results at the translational level (Figure 3J). Altogether, the data show that the stem-II-based *cis*-acting aptazymes obtained through intracellular selection can be utilized as *trans*-acting tools to knock down endogenous genes in the presence of theophylline regulator.

To explore the potential of T195 as a conditional knockdown tool, we further investigated and optimized the *trans*-acting aptazyme. First, four theophylline analogs, including caffeine, adenine, xanthine, and hypoxanthine, were used to induce the downregulation of p65 in MCF-7 cells expressing T195. As shown in Figures 4A and S20, only theophylline triggered a significant decrease of p65 protein, even though their molecular structures are very similar, revealing the high specificity of *trans*-acting aptazyme to its small-molecule regulator. To further improve the knockdown ability of our *trans*-acting aptazyme, two T195 targeting p65 (D195) were added to the same transcript, which would be transcribed and processed by U6-tRNA system to get more knockdown tools (Figures 4B and S21). We found that much higher downregulation (73.5%) of p65 was achieved by D195 compared to T195 (47.2%) with 1 mM theophylline in MCF-7 cells (Figures 4C and S22), revealing that the knockdown efficiency could be tuned by the introduction of multiple aptazymes. Owing to the small size (~60 nt in length), the *trans*-acting T195 can be transcribed or synthesized *in vitro* easily. Therefore, we prepared T195 RNA tools (targeting p65) *in vitro* and transfected them into MCF-7 cells with liposomal transfection reagent. We found that the synthetic aptazymes T195 functioned properly and induced the downregulation of p65 in the presence of theophylline more quickly compared to genetically expressed T195 (Figures 4D and S23).

DISCUSSION

Without permanent modification of genetic code, RNA knockdown provides a much safer approach for genetic therapies through turning off the target genes causing the disease, which could avoid the risks and concerns associated with DNA-based gene therapies. In these applications, the conditional knockdown tools based on *trans*-acting aptazymes offer unique features. (1) External control of the specific in cancer cells knockdown could be realized with a small-molecule ligand, which induces the *trans*-cleavage of target mRNA by a ligand-dependent hammerhead ribozyme. (2) To knock down a given gene, both binding arms of *trans*-cleaving hammerhead ribozymes need to be complementary to the target mRNA simultaneously, and the cleaving site in the mRNA substrate needs to fulfill "NUH↓" rule, coupled with the existence of small-molecule ligands. The new tools are therefore highly specific, with few off-target effects. (3) The *trans*-acting aptazyme is composed entirely of RNA, which can perform its function without help from any proteins and has no immunogenicity. (4) Due to the small size, *trans*-acting aptazymes can be synthesized and chemically modified easily or included in gene therapy vectors such as AAV with limited space for additional genes. Therefore, an intracellular selection of stem II-based *cis*-acting hammerhead aptazymes was carried out by us, through which three theophylline-dependent *cis*-acting aptazymes were obtained. Fortunately, those *cis*-acting aptazymes can be utilized as specific *trans*-acting tools for conditional downregulation of target genes in

eukaryotic cells directly. Unlike interfering RNA, which achieves more efficient gene knockdown with the assistance of the RISC complex, aptazymes rely on their own catalytic activity to accomplish the targeted gene knockdown. As a result, aptazymes provide faster gene knockdown; however, they exhibit lower knockdown efficiency and reduced stability in cells due to their RNA composition.

Overall, these experiments provide compelling evidence for the effectiveness of intracellular selection in obtaining *trans*-acting aptazymes. This selection strategy has great potential for developing additional stem II-based hammerhead aptazymes that respond to different molecules. Of the aptazymes examined in this study, T195, a single-stranded RNA molecule of approximately 60 nucleotides, demonstrated the most potent knockdown ability on endogenous genes in the presence of theophylline, with a consistent and improved performance. Using T195 as a novel molecular tool, we were able to achieve conditional suppression of *RELA* and *VEGFA* genes in cancer cells with theophylline, a commonly used and safe medication. The knockdown effect of T195 was specifically regulated by theophylline in a dose-dependent and time-dependent manner, and the knockdown efficiency could be further improved by expressing multiple copies of T195. These results demonstrate that the *trans*-acting aptazyme T195 is a useful, controllable RNA-targeting knockdown tool for both research and therapeutic purposes due to its small size, safety, and tunable properties.

MATERIALS AND METHODS

Cells and reagents

High fidelity restriction endonucleases BamHI-HF, HindIII-HF, EcoRI-HF, XbaI-HF, and T4 ligase enzyme were purchased from NEB (New England Biolabs, MA, USA). Bacteria strain DH10B, BL21(DE3), Taq DNA polymerase, and All-in-One First-Strand cDNA Synthesis SuperMix for qPCR were purchased from Transgen, and JM109(DE3) was purchased from Promega (Promega, WI, USA). pT7Oi and pT7Om vectors were already constructed by our group. psilence-2.1-U6-Hygro vector was purchased from Beijing Rambolide Trading Co. DNA fragments were purified with AxyPrep DNA Gel Extraction Kit (Axygen) or DNA Clean-up Kit (Cwbio), and plasmids were extracted by FastPure Plasmid Mini Kit (Vazyme) or Endo-Free Plasmid Mini Kit I (Omega). Cell RNA Kit, BCA protein quantification kit, and Hieff Trans liposomal transfection reagent were purchased from Yeasen. ProtLytic Protein Lysis and Sample Loading was purchased from New Cell & Molecular biotech Co. Human embryonic kidney 293T (HEK293T) was a gift from Professor Yao Shaohua's laboratory. Michigan Cancer Foundation-7 (MCF-7) and human hepatocellular carcinomas (Hep G2) were purchased from ATCC (American Type Culture Collection, VA, USA).

Library design and construction

The DNA sequence of the selection pool was as follows: 5′-GGAATCCA GCTGATGA(N2-4)ATACCAGCCGAAAGGCCCTTGGCAG(N2-4) GAAACGCGCTTCGGCGCGTCCTGGATTCCG-3′. N2-4 is 2–4 randomized nucleotides in linker module, and the DNA sequences are shown in the supplemental information (Table S1). The selection dsDNA pools were prepared from fusion PCR, and primers are shown in the supplemental information (Table S2). Fusion PCR was performed as follows: pre-denaturation at 95°C for 1 min and then 30 cycles (30 s at 95°C, 30 s at 55°C, 30 s at 72°C of each cycle). The DNA fragments were purified with AxyPrep DNA Gel Extraction Kit and then digested with restriction enzymes BamHI-HF and HindIII-HF at 37°C for 3 h and purified with DNA Clean-up Kit. The selection vector pT7Oi was also digested with same restriction enzymes at 37°C for 3 h, and purified with AxyPrep DNA Gel Extraction Kit. The digested DNA fragment and vector were ligated with NEB T4 ligase at 16°C for 24 h, and then the purified ligase product was transformed into JM109(DE3) by electrochemical transformation. After recovering at 225 rpm/min for 1 h, bacteria were coated on the resistant culture plate with 100 μg/mL ampicillin, 1 mM IPTG, and theophylline.

Intracellular selection and definition of hammerhead aptazymes in bacteria

Bacteria harboring DNA selection pools were cultivated on the resistant culture plate, and those that survived the resistant medium were picked and sequenced. After sequencing, we selected those with the correct sequence for the next selection. Then we extracted these candidate plasmids with the FastPure Plasmid Mini Kit, transformed into JM109 (DE3) at 42°C for 90 s, and then incubated at 150 rpm/min for 1 h, and 50 μL of each was coated on the solid Luria-Bertani (LB) plates with and without theophylline independently. After culturing at 37°C for 24 h, the bacterial growth on different LB plates was observed. Those that grew better on LB plates containing theophylline than those without theophylline were selected for further study. After obtaining stem II-based theophylline-dependent hammerhead ribozymes, to quantify the cleavage efficiency, we employed the pT7Om vector, which replaced the toxin protein IbsC with the fluorescent protein mCherry on the selection pT7Oi vector. All stem II-based theophylline-dependent hammerhead ribozymes were constructed into pT7Om. These plasmids were extracted and transformed into BL21 (DE3). More than three single clones of each construct were picked and grown in 5 mL of LB liquid medium containing ampicillin at 250 rpm/min at 37°C, until the OD600 of the medium reaches 0.3, when the bacteria were in the logarithmic growth phase, and the medium was then divided into two parts, one with IPTG (final concentration 1 mM) and one with IPTG (final concentration 1 mM) and theophylline (final concentration 1.25 mM), incubated at 150 rpm/min at 37°C for 18 h. Bacteria were then collected and centrifuged at 4,000 rpm/min for 5 min, washed twice with PBS buffer, and then resuspended in 500 μL PBS buffer and analyzed by flow cytometry (excitation wavelength 561 nm, emission wavelength 610 nm). For dose-dependent experiments, bacteria containing theophylline-dependent hammerhead ribozyme T195 were induced with different concentrations of theophylline. Experiments were repeated at least three times independently.

In vitro cleavage activity of hammerhead aptazymes

The sequence of 3′FAM-labeled substrate was as follows: 5′ CGAAUGGCUCGUCUGUAGUGCA 3′. The reaction was performed in 50 mM Tris-HCl (pH 7.5) buffer containing 1 mM

$MgCl_2$, 150 mM KCl, and 1 mg/mL BSA at 37°C for 10 min with or without theophylline. The reaction products were purified by 20% denaturing polyacrylamide gel. Experiments were repeated at least three times independently.

Knocking down endogenous genes by hammerhead aptzymes in cancer cells

To further validate the *trans*-cleavage ability of stem II-based theophylline-dependent hammerhead ribozymes, we performed endogenous gene-targeting experiments in cancer cells. We employed the psilence-2.1-U6-Hygro vector, whose structure is shown in Figure S24. We designed ribozyme DNA sequences targeting *RELA* mRNA, synthesized by Sangon Biotech, and then constructed into psilence-2.1-U6-Hygro vector. After obtaining these recombinant vectors by sequencing analysis, we extracted these plasmids by Endo-Free Plasmid Mini Kit. 2.5 μg/well of recombinant plasmids containing different *trans*-aptazymes was parallelly transfected into MCF-7 cells in six-well plates with Hieff Trans in the presence and absence of theophylline. After transfection for 24 h, the total protein of MCF-7 cells was extracted by ProtLytic Protein Lysis and Sample Loading, and its concentration was determined with BCA protein quantification kit, and the expression of p65 was analyzed by WB. Meanwhile, we investigated the knockdown ability of *trans*-acting aptazymes on *RELA* mRNA level by real-time qRCR. After transfection for 24 h, the total RNA of MCF-7 cells was extracted by Cell RNA Kit and reverse transcribed to cDNA by All-in-One First-Strand cDNA Synthesis SuperMix for qPCR (One-Step gDNA Removal), and then the expression of *p65* was analyzed by real-time qRCR, the primers are shown in the supplemental information (Table S3). Real-time qRCR was performed as follows: pre-denaturation at 95°C for 10 min and then 40 cycles (15 s at 95°C, 15 s at 58°C, 15 s at 72°C of each cycle). Experiments were repeated at least three times independently.

Specifically knocking down endogenous gene *RELA* by aptazyme T195 in cancer cells

To test the specificity of *trans*-acting T195, we tested four theophylline analogs, caffeine, adenine, xanthine, and hypoxanthine, and 2.5 μg/well of plasmids containing *trans*-acting T195 was transfected into MCF-7 cells in the presence of different small molecules. After transfection for 24 h, the total protein of MCF-7 cells was extracted, and p65 was analyzed by WB. Experiments were repeated at least three times independently.

Knocking down endogenous gene *RELA* by T195 RNA in cancer cells

The sequence of T195 RNA was as follows: 5′-UGCACUACAGACC UGAUGAGUAUACCAGCCGAAAGGCCCUUGGCAGACGAAA GCCAUUCG-3′. The 2′OH on ribose of the first uracil ribonucleotide at the 5' end and the 2′OH on ribose of the first guanine ribonucleotide at the 3′ end were both methoxy modified. The RNA was synthesized by Qingke Biotechnology Co. 1 μg/well of T195 RNA was transfected into MCF-7 cells in six-well plates with Hieff Trans in the presence and absence of theophylline. After transfection for 5, 7, or 9 h, the total protein of MCF-7 cells was extracted, and p65 was analyzed by WB. Experiments were repeated at least three times independently.

Statistical analysis

Results were expressed as mean ± SD, with one-way ANOVA multiple comparisons for all samples.

DATA AND CODE AVAILABILITY

The data that support the findings of this study are available on request from the corresponding author, upon reasonable request.

SUPPLEMENTAL INFORMATION

Supplemental information can be found online at https://doi.org/10.1016/j.omtn.2023.07.014.

ACKNOWLEDGMENTS

This research was funded by the Youth Innovation Promotion Association CAS 2020365; Chengdu Municipal Bureau of Science and Technology 2021-YF05-01739-SN; National Natural Science Foundation of China 21877108, 21907090 and 22177111; Sichuan Science and Technology Program 2022YFS0012, 2022YFS0432, and 2022ZYD0090, and Sichuan Medical Research Program S20005.

AUTHOR CONTRIBUTIONS

Z.T. conceived and provided guidance and suggestions and optimized rationally. S.Z. designed and performed the experiments and interpreted results. S.Z., M.C., Y.Y., Y.X., Q.P., X.A, S.L., F.D., X.H, J.D., and X.C. performed experiments and data analysis. S.Z. and Z.T. prepared the figures and wrote the manuscript. All authors read and approved the paper.

DECLARATION OF INTERESTS

The authors declare no competing interests.

REFERENCES

1. Fedor, M.J., and Uhlenbeck, O.C. (1992). Kinetics of intermolecular cleavage by hammerhead ribozymes. Biochemistry *31*, 12042–12054.
2. Martick, M., and Scott, W.G. (2006). Tertiary Contacts Distant from the Active Site Prime a Ribozyme for Catalysis. Cell *126*, 309–320.
3. Prody, G.A., Bakos, J.T., Buzayan, J.M., Schneider, I.R., and Bruening, G. (1986). Autolytic Processing of Dimeric Plant Virus Satellite RNA. Science *231*, 1577–1580.
4. Akashi, H., Matsumoto, S., and Taira, K. (2005). Gene discovery by ribozyme and siRNA libraries. Nat. Rev. Mol. Cell Biol. *6*, 413–422.
5. Burnett, J.C., and Rossi, J.J. (2009). Stem cells, ribozymes and HIV. Gene Ther. *16*, 1178–1179.
6. Bao Chi, W., Umama, S., and Hock Siew, T. (2022). Ribozymes as Therapeutic Agents Against Infectious Diseases. In RNA Therapeutics - History, Design, Manufacturing, and Applications, L. Irina Vlasova-St, ed. (IntechOpen). Ch. 6.
7. Huang, X., Zhao, Y., Pu, Q., Liu, G., Peng, Y., Wang, F., Chen, G., Sun, M., Du, F., Dong, J., et al. (2019). Intracellular selection of trans-cleaving hammerhead ribozymes. Nucleic Acids Res. *47*, 2514–2522.
8. Wieland, M., and Hartig, J.S. (2008). Improved Aptazyme Design and In Vivo Screening Enable Riboswitching in Bacteria. Angew Chem. Int. Ed. Engl. *47*, 2604–2607.

9. Win, M.N., and Smolke, C.D. (2007). A modular and extensible RNA-based gene-regulatory platform for engineering cellular function. Proc. Natl. Acad. Sci. USA *104*, 14283–14288.
10. Ausländer, S., Ketzer, P., and Hartig, J.S. (2010). A ligand-dependent hammerhead ribozyme switch for controlling mammalian gene expression. Mol. Biosyst. *6*, 807–814.
11. Wittmann, A., and Suess, B. (2011). Selection of tetracycline inducible self-cleaving ribozymes as synthetic devices for gene regulation in yeast. Mol. Biosyst. *7*, 2419–2427.
12. Klauser, B., Atanasov, J., Siewert, L.K., and Hartig, J.S. (2015). Ribozyme-Based Aminoglycoside Switches of Gene Expression Engineered by Genetic Selection in S. cerevisiae. ACS Synth. Biol. *4*, 516–525.
13. Townshend, B., Kennedy, A.B., Xiang, J.S., and Smolke, C.D. (2015). High-throughput cellular RNA device engineering. Nat. Methods *12*, 989–994.
14. Beilstein, K., Wittmann, A., Grez, M., and Suess, B. (2015). Conditional Control of Mammalian Gene Expression by Tetracycline-Dependent Hammerhead Ribozymes. ACS Synth. Biol. *4*, 526–534.
15. Zhong, G., Wang, H., Bailey, C.C., Gao, G., and Farzan, M. (2016). Rational design of aptazyme riboswitches for efficient control of gene expression in mammalian cells. Elife *5*, e18858.
16. Pu, Q., Zhou, S., Huang, X., Yuan, Y., Du, F., Dong, J., Chen, G., Cui, X., and Tang, Z. (2020). Intracellular Selection of Theophylline-Sensitive Hammerhead Aptazyme. Mol. Ther. Nucleic Acids *20*, 400–408.
17. Jacobs, M.H., Senior, R.M., and Kessler, G. (1976). Clinical Experience With Theophylline: Relationships Between Dosage, Serum Concentration, and Toxicity. JAMA *235*, 1983–1986.
18. Mok, W.W.K., and Li, Y. (2013). A Highly Efficient Molecular Cloning Platform that Utilises a Small Bacterial Toxin Gene. Chembiochem *14*, 733–738.
19. Fozo, E.M., Makarova, K.S., Shabalina, S.A., Yutin, N., Koonin, E.V., and Storz, G. (2010). Abundance of type I toxin–antitoxin systems in bacteria: searches for new candidates and discovery of novel families. Nucleic Acids Res. *38*, 3743–3759.
20. Fozo, E.M., Kawano, M., Fontaine, F., Kaya, Y., Mendieta, K.S., Jones, K.L., Ocampo, A., Rudd, K.E., and Storz, G. (2008). Repression of small toxic protein synthesis by the Sib and OhsC small RNAs. Mol. Microbiol. *70*, 1076–1093.
21. Soukup, G.A., Emilsson, G.A., and Breaker, R.R. (2000). Altering molecular recognition of RNA aptamers by allosteric selection11Edited by D. E. Draper. J. Mol. Biol. *298*, 623–632.
22. Soukup, G.A., and Breaker, R.R. (1999). Engineering precision RNA molecular switches. Proc. Natl. Acad. Sci. USA *96*, 3584–3589.
23. Santoro, S.W., and Joyce, G.F. (1997). A general purpose RNA-cleaving DNA enzyme. Proc. Natl. Acad. Sci. USA *94*, 4262–4266.
24. Ghosh, S., May, M.J., and Kopp, E.B. (1998). NF-κB AND REL PROTEINS: Evolutionarily Conserved Mediators of Immune Responses. Annu. Rev. Immunol. *16*, 225–260.
25. Taniguchi, K., and Karin, M. (2018). NF-κB, inflammation, immunity and cancer: coming of age. Nat. Rev. Immunol. *18*, 309–324.
26. Xie, K., Minkenberg, B., and Yang, Y. (2015). Boosting CRISPR/Cas9 multiplex editing capability with the endogenous tRNA-processing system. Proc. Natl. Acad. Sci. USA *112*, 3570–3575.
27. Brown, K., Park, S., Kanno, T., Franzoso, G., and Siebenlist, U. (1993). Mutual regulation of the transcriptional activator NF-kappa B and its inhibitor, I kappa B-alpha. Proc. Natl. Acad. Sci. USA *90*, 2532–2536.
28. Huang, S., Pettaway, C.A., Uehara, H., Bucana, C.D., and Fidler, I.J. (2001). Blockade of NF-κB activity in human prostate cancer cells is associated with suppression of angiogenesis, invasion, and metastasis. Oncogene *20*, 4188–4197.
29. Tang, J., and Breaker, R.R. (1997). Rational design of allosteric ribozymes. Chem. Biol. *4*, 453–459.
30. Soukup, G.A., and Breaker, R.R. (1999). Design of allosteric hammerhead ribozymes activated by ligand-induced structure stabilization. Structure *7*, 783–791.
31. Claesson-Welsh, L., and Welsh, M. (2013). VEGFA and tumour angiogenesis. J. Intern. Med. *273*, 114–127.